FRACTURE PROPERTIES FROM SEISMIC SCATTERING

by

Daniel R. Burns, Mark E. Willis, Laura Vetri (ENI-Agip), and M. Nafi Toksöz

Earth Resources Laboratory
Department of Earth, Atmospheric, and Planetary Sciences
Massachusetts Institute of Technology
Cambridge, MA 02139

Abstract

Fractures scatter seismic energy and this energy can be analyzed to provide information about fracture direction and density. Laboratory and numerical (finite difference) models of fractures show that scattered energy varies with the seismic acquisition direction relative to the orientation of parallel fracture sets. Data acquired normal to fracture strike displays forward and backscattered energy that is canceled in the stacking process, while data acquired parallel to the fracture strike contains forward scattered and guided waves that are enhanced by stacking. The Scattering Index method estimates the fracture orientation by comparing wavelet changes in the data from azimuthal stacks. Fracture density or spacing can be estimated by spectral methods that include f-k analysis of backscattered energy or analysis of spectral notches as functions of azimuth. Application of these methods to data from a fractured carbonate field results in fracture orientation and density estimates that are consistent with borehole measurements.

II. Introduction

The seismic trace is a complex aggregate of reflected and scattered signals from subsurface formation interfaces and heterogeneities. Although many varieties of random noise may also be present in the trace, we know from reacquiring the same seismic survey that seismic data are highly repeatable, indicating that significant information about the subsurface is contained in the trace yet not used by our standard analysis methods. Seismic scattering is a type of signal contained in the data that is generally not utilized. Most of our processing methods are focused on optimizing the specular reflections from subsurface lithology or fluid boundaries for structural and stratigraphic interpretation. The presence of small-scale heterogeneities, creating variability in seismic properties that are on the order of a wavelength or less, will also generate seismic signatures. However, the scattered signals will appear to be less coherent and not be correlated over long distances. Such signals are generally treated as 'random noise' in the sense that stacking and deconvolutional processes may effectively remove them in many situations. Because these signals contain information about the subsurface at smaller scales it would be beneficial to find ways to extract and utilize them. One particular application where this is true is in the area of fracture characterization. Fractures can cause significant scattering since they generally have large contrasts in elastic properties compared to the surrounding rock. In addition this contrast will be greatest for those fractures that 'open', and therefore have the largest impact on reservoir productivity. Although fractures may exist with a variety of orientations in the subsurface due to changing stress regimes over time, those fractures that are oriented

1

parallel to the present day maximum horizontal stress direction will be open and generate the most scattering. Over the past several years we have developed several methods for using scattered seismic energy to extract information about subsurface fractures. In this paper we will give an overview of these methods, which can provide estimates of fracture orientation and spacing, and show a field application to a fractured carbonate reservoir. We are now looking to apply these ideas to the characterization of induced (hydro-) fractures. The integration of seismic scattered wave analysis with microseismic monitoring data could provide a way to estimate hydrofrac properties away from the well from surface or VSP data.

Background: Scattering observations in the lab and numerical modeling

The use of the scattered wavefield to study heterogeneity in the Earth has received much attention in the earthquake seismology field (e.g., Aki and Chouet, 1975; Frankel and Clayton, 1986; Sato and Fehler, 1998). In exploration applications, however, most of the focus has been on removing scattered arrivals rather than extracting information from them. Simple numerical models provide some insight in the effects of small-scale heterogeneity on the wavefield. For example, propagation through a random distribution of velocity heterogeneity filtered by a Gaussian correlation function with a prescribed correlation scale length results in scattered wave energy creating a coda behind the direct arrival. Spectral analysis of the scattered energy in such models can provide statistical information about the heterogeneity distribution (e.g., Frankel and Clayton, 1986; Jannaud et al., 1993). For example, since maximum scattering occurs when the heterogeneity size is approximately equal to the wavelength, the spectral peak of the scattered field can provide an estimate of the correlation scale length. Figure 1a shows the variations in the spectral peak frequency for models with different heterogeneity correlation scale lengths (from 2 to 20 m). The spectral amplitude will be sensitive to the scattering strength, which is proportional to the velocity or impedance contrast of the heterogeneities (Figure 2b).
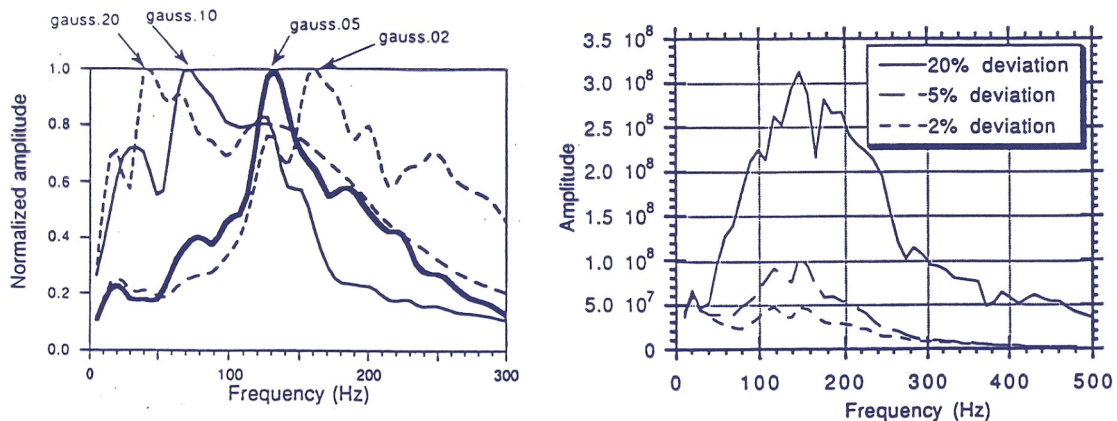

Figure 1 Spectral analysis of scattered wave energy from 2D numerical models of random (Gaussian) heterogeneity. The average spectra show a shift in the peak frequency that is a function of the correlation length of the heterogeneity (left panel) and an increase in scattered wave amplitude as the contrast between the background velocity and heterogeneity velocity increases (right panel).

Fractures can impose similar characteristics on a seismic signal in that the scattered wavefield will be a function of the fracture spacing (scale) as well as the fracture compliance (e.g., Pyrak-Nolte, 1996). Because fractures are elongated linear features, however, the scattering will also have strong directional characteristics. Laboratory scale model results provide an effective illustration of these effects (Schultz and Toksöz, 1995; Groenenboom and Falk, 2000; Luo and Evans, 2004). Figure 2a shows a schematic representation of a physical model used in an ultrasonic lab experiment by Schultz and Toksöz (1995). In this experiment, an aluminum block has a series of parallel grooves scratched into the surface simulating the effect of vertical parallel fractures. This fracture analog model was then placed in a water tank and an acoustic source and receiver located above the block was used to collect a shot gather across the sample. Figure 2b shows a finite difference model snapshot of the wavefield expected for this experiment. Note the scattered coda energy that follows the reflected wave front from the top of the block. This coda contains both forward and backscattered energy for this acquisition direction, which is perpendicular to the 'fracture' strike direction.

Figure 2 A schematic of the laboratory model used by Schultz and Toksöz (1995) to study scattering from an aluminum block with parallel grooves cut into the surface (left panel). The right panel shows a wavefield snapshot from a finite difference model of the aluminum block. Note the scattered wave energy that follows the reflection from the top of the block.

The results of the physical experiment confirm these numerical results. Figure 3a and 3b shows the shot gather acquired perpendicular and parallel to the grooves, respectively. Notice that in the perpendicular case both forward and backscattered energy is seen, while in the parallel case only forward scattering exists. In both cases the scattered energy exists as a coda following the main reflection off the block. In the perpendicular direction backscattered energy (i.e., propagating back towards the source) is generated by the wavefront interacting with the grooves. In the parallel direction the wavefront is guided by the parallel grooves creating a long series of forward scattered arrivals.
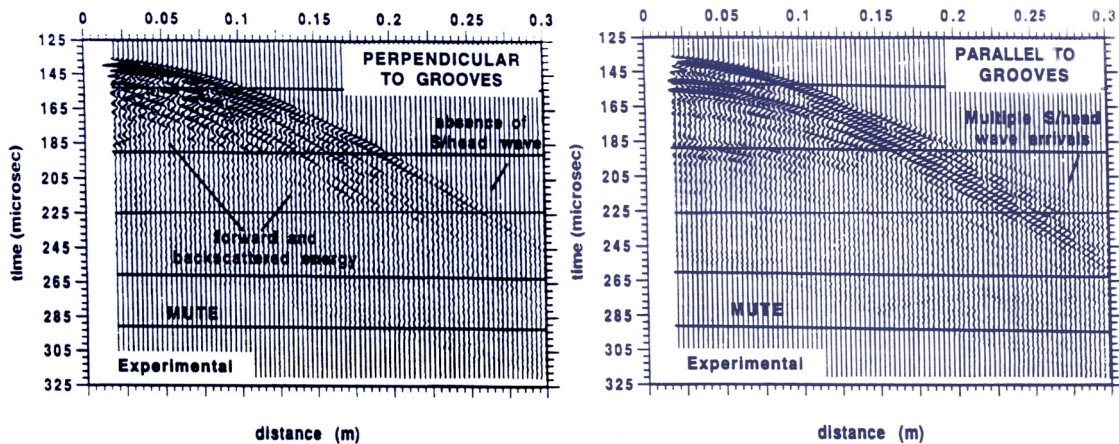
Figure 3 Laboratory acoustic data acquired over the aluminum block model shown in Figure 2. Left panel shows the data acquired normal to the strike of the grooves and the right panel shows the data acquired parallel to the strike. Note that backscattered energy can be seen when the data are perpendicular to the grooves, while only forward scattered energy is seen parallel to the grooves. (From Schultz and Toksöz, 1995)

These numerical and physical modeling results suggest several ways for us to extract fracture properties from seismic scattered data: 1) azimuthal variations in the scattered wavefield can provide estimates of fracture orientation, 2) the amount of backscattered energy can also provide an indicator of orientation, and 3) spectral analysis can provide estimates of fracture spacing and compliance. The use of scattered wave methods to estimate fracture properties is very different from conventional AVO type analyses, providing an independent means of validating results. In addition, as we will show below, some of our proposed methods use a differential analysis (comparison of coda energy in different time windows) that can eliminate acquisition footprints and overburden effects, which may make such analysis preferable to AVO-based methods.

Fracture systems – numerical models and analysis methods

A system of aligned fractures affects propagating seismic waves in several ways. If the fracture size and spacing are small relative to the seismic wavelength, then the fractures cause the reservoir rock to behave like an equivalent anisotropic medium with a symmetry axis normal to the strike of the 'open' fractures. The resulting seismic anisotropy will therefore be related to the fluid flow directions in the reservoir. We can develop analysis methods to estimate the orientation of these open fractures as well as the fracture density from seismic measurements. In particular, seismic reflections from the top and bottom of a fractured reservoir will display different amplitude variations with offset (AVO) as a function of the orientation of the seismic source-to-receiver direction relative to the orientation of the fractures. Such measurements are referred to as amplitude variations with offset and azimuth (AVOA). This is a well-developed method of fracture analysis from seismic data (e.g., Lynn et al., 1996; Mallick et al., 1998; Ruger, 1998).

If, however, the fractures and fracture spacing are closer in size to the seismic wavelength, then the fractures will scatter the seismic energy causing a more complex seismic signature (Nihei et al., 2002; Nakagawa et al., 2003; Vlastos et al., 2003; Willis et al., 2004). These larger scale features are the major fracture corridors within a reservoir. Such features will control the majority of flow within the reservoir and therefore are critical to reservoir performance. The scattered wave energy results in a seismic signature that varies as a function of the orientation of the seismic acquisition relative to the fracture orientation, providing information about the fracture orientation and spacing or density.

In much the same way that we saw the scattered wave signals in the grooved aluminum block, we see a similar effect when we use finite difference modeling to predict the seismic response of a series of parallel fractures. Figure 4 shows the input model, and a wavefield snapshot oriented perpendicular to the fracture strike. The reverberating scattered energy due to the fractures is clearly seen.
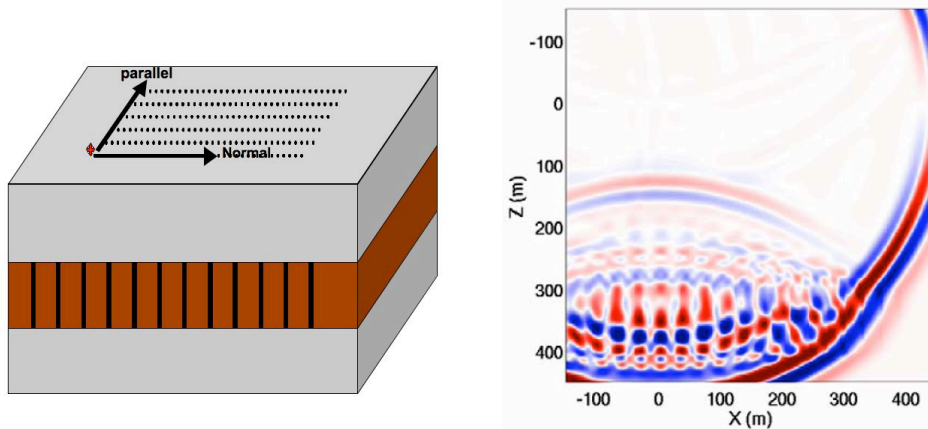

Figure 4 A simple layered model with vertical, parallel fractures contained in the middle layer (left panel). A wavefield snapshot for a slice oriented normal to the fracture strike (right panel). Note the scattered wave energy due to the fractures.

Using a 3-D elastic, anisotropic, rotated staggered grid (RSG), finite difference code (Saenger, 2004) to model fractured reservoirs (Zhang et al., 2006), and the method of Coates and Schoenberg (1995) to represent the presence of fractures within a given finite difference cell, we developed a range of simple models where a fractured reservoir is represented as a homogeneous background medium containing parallel vertical fracture zones separated by different amounts of spacing. Each fracture zone is one grid cell wide (5 m grid size in these models), with the properties of each grid cell derived from the Coates-Schoenberg formulation. These grid cells can be thought of as a fracture zone, or corridor, containing thin fractures. The compliance of the cell (fracture compliance) controls the amount of scattering, the more compliant the cell, the greater the scattering. Although most of our models were based on a single set of parallel vertical fractures, we also investigated the effect of multiple fracture sets on seismic scattering. The Coates-Schoenberg formulation is quite general as it allows for modeling multiple intersecting sets of fractures with arbitrary orientations. However, in order to fully benefit from this

flexibility, the finite-difference code must allow for fairly arbitrary anisotropy (at least monoclinic).

Our canonical fractured reservoir model consists of a simple reservoir geometry consisting of five horizontal layers. All the layers except for the third layer are homogeneous and isotropic elastic media. The third layer is 200-m thick and contains parallel, vertical fractures that are as tall as the layer, one grid cell thick (5m), and run the entire width of the model (Figure 5). We generated a series of models with fracture spacing ranging from 10m to 100m. More complex models were also considered: one with two sets of fractures with different spacing and orientation, and the other with a Gaussian distribution of spacing. All models use a 40Hz Ricker wavelet as the seismic source (P wavelength of 100m and S wavelength of 60m).
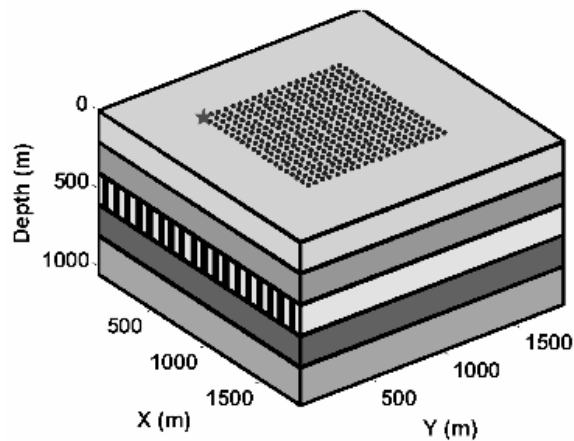

Figure 5 The geometry used for a suite of fractured reservoir finite difference models. All fractures are contained in the third layer.
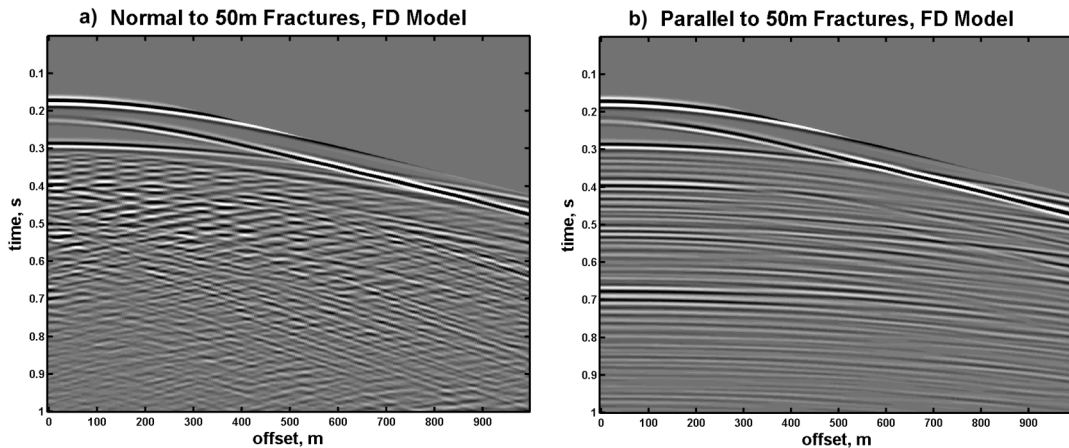

Figure 6. Vertical component of the 3D Finite difference modeling for 50m fracture spacing; a) shows the shot record acquired normal to the fractures, b) shows the shot record acquired parallel to the fracture direction. Note the presence of backscattered energy in the normal direction (a).

Figure 6 shows the results for a model with a single set of vertical fractures with 50m spacing. The seismic shot gather oriented normal to the fractures shows complex forward and back-scattering below the reservoir level, while the shot gather parallel to the fractures shows a more organized semi-parallel set of arrivals consisting of forward scattering and multiplied scattered waves that are guided along the fracture strike. It is this difference in scattering as a function of orientation that can be exploited to estimate fracture orientation.

The Scattering Index Method (Willis et al., 2006) is based on the observation that if we perform normal moveout corrections and stack the data shown in Figure 6, the scattered energy will be canceled out by the stacking process when we the data are oriented normal to the fractures, but the scattered energy will be enhanced when the data are oriented parallel to the fractures. To test this hypothesis we generated synthetic shot gathers at ten-degree azimuthal increments, ranging from 0 to 90 degrees relative to the fracture normal direction. The azimuthal stacks (Figure 7a) show that the stacked trace contains significant coda energy only in the direction parallel to the fractures.

These scattered coda arrivals will not be easily seen in field data because of the complex distribution of reflectivity in the subsurface. In addition, if there are fractured zones or other scatterers in the overburden, those scattered waves will contaminate, or overprint, the scattered energy from any zone of interest in the reservoir. With these issues in mind, Willis et al. (2006) developed a differential deconvolutional method to analyze the seismic scattering. The analysis approach calculates the autocorrelations from windowed portions of the reflection time series to estimate two local source wavelets from the reflection time series – one above the fractured zone (the "input" wavelet) and one below it (the "output" wavelet). A transfer function is then computed by deconvolving the input wavelet from the output wavelet. This transfer function characterizes the effect of scattering in the interval of interest, between the two windowed portions of the trace. A simple pulse shaped transfer function indicates no scattering, while a long oscillatory transfer function captures the scattering within the reservoir interval. It is important to note that any contamination from scattering above the interval will be present in both the input and output extracted wavelets and thus will be excluded from the transfer function. If the method is applied to data stacked in different azimuthal directions, the interval transfer function should exhibit greater ringing in the direction parallel to fracturing. Figure 7b shows the transfer functions derived for the stacked traces in the Figure 7a. We can see that the transfer functions are all compact and similar to the non-fractured case (labeled "control") for orientations that are not parallel to the fractures. However, for azimuthal stacks oriented parallel to the fractures, the transfer function contains significant energy at non-zero lag values.
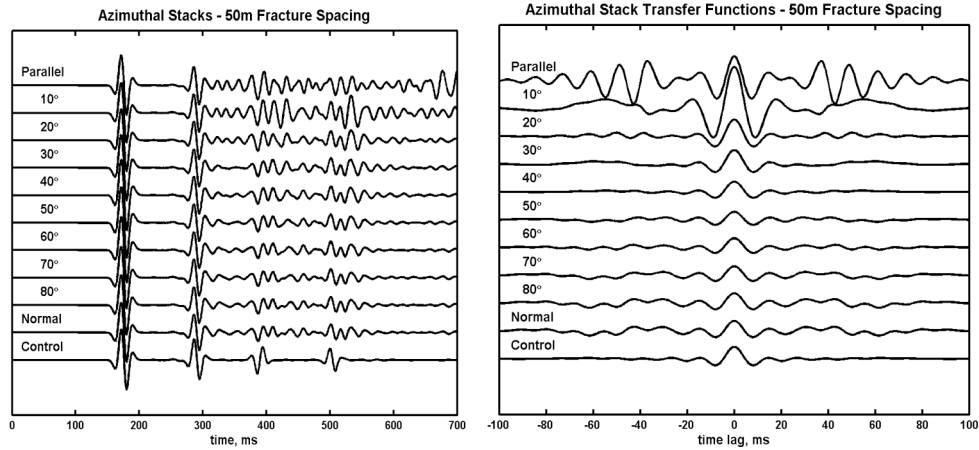
Figure 7. Left Panel: a plot showing the azimuthal stacks of traces from the 50m fracture spacing model. The traces represent azimuth stacks starting in the direction parallel to fracturing (top), and then increasing in 10-degree increments until normal to the fractures. The bottom trace shows the stack for the model without a fractured layer. Right panel: a plot showing the transfer functions corresponding to the azimuthal stacks in the left panel.

The Scattering Index value, which provides a simple attribute measure, is the sum of the rectified transfer function values preferentially weighting the non-zero lags (Willis et al., 2006). This methodology has two important characteristics. First, the method is robust and computationally inexpensive, and second, the method uses a normalization or differential approach that compares the scattering signal above and below an interval of interest in the data. As a result, the method should remove any overburden or acquisition footprint from the resulting estimates (a concern with AVOA results).
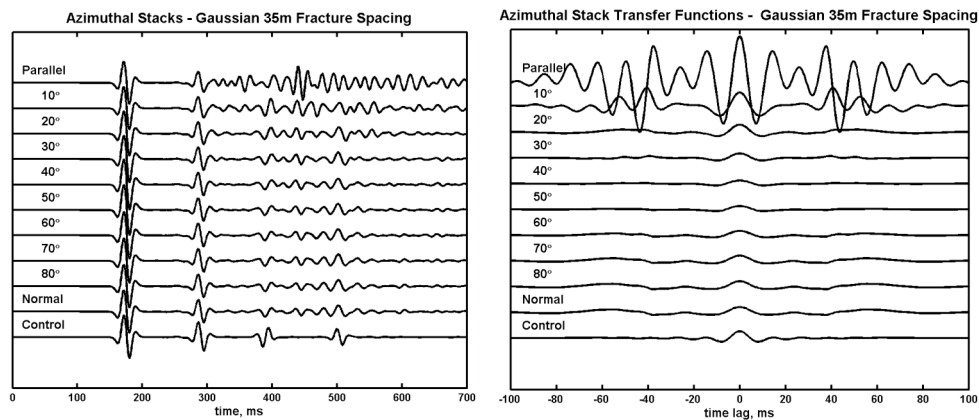

Figure 8 Left panel: azimuthal stacks for a model with a Gaussian distribution of fracture spacing with a mean of 35m and a standard deviation of 10m. Right panel: the transfer functions corresponding to the same stacks.

For a single set of aligned fractures with different spacing the azimuthal stacks show consistently strong scattering in the direction parallel to the fracture strike. We also tested the approach on models with non-regular spacing of fractures as well as with multiple sets of fractures. In both cases the approach shows similar results. Figure 8 shows the azimuthal stacks and transfer functions for a model with one set of parallel fractures with a Gaussian distribution of fracture spacing (mean of 35m and standard deviation of 10m). Multiple fracture sets also show similar behavior. Figure 9 shows the azimuthal stacks and resulting scattering index values for a model with two sets of orthogonal fractures with different fracture spacing values (35m and 50m). The Scattering Index values clearly show the fracture orientation and the amplitude of the values gives an indication of the spacing (or fracture density) differences (note: differences in the fracture compliance could cause similar variations in Scattering Index values).
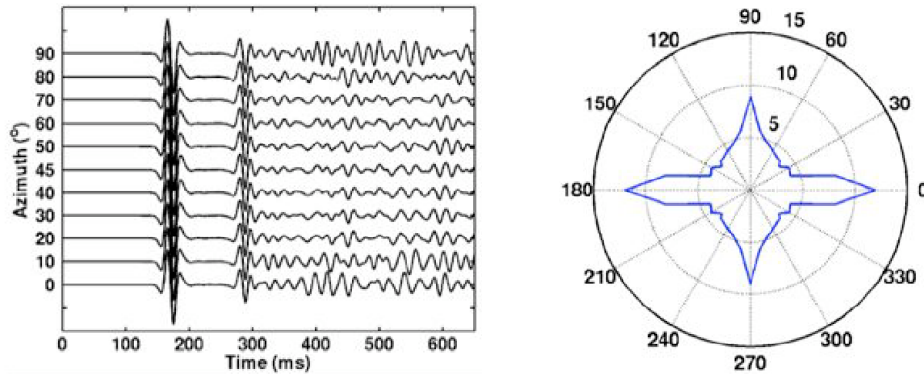

Figure 9. Azimuthal stacks (left) and Scattering Index values (right) for a model with two orthogonal fracture sets with same compliance but different spacing. The fractures at 0 degrees are spaced at 35m, while the fractures at 90 degrees spaced at 50m.

Fracture spacing is another important parameter in reservoir development. There are two approaches for estimating fracture spacing from scattered seismic energy in pre-stack data. The first relates notches in the amplitude spectra of the scattered wavefield to the dominant fracture spacing that caused the scattering (Willis et al., 2005). The second uses conventional FK filtering to isolate the backscattered signals and then recovers an estimate of the fracture spacing from the dominant wavelength of those signals (Zhang et al., 2006). The first method is based on the observation that discrete, vertically aligned fracture systems impart one or more notches in the spectral ratios of stacked reflected seismic traces. This apparent attenuation is due to the azimuth dependant scattering introduced by the fractures. The most prominent notch is located at the frequency where the P wavelength is about twice the fracture spacing. The frequency location of the notches can be used to determine the fracture spacings. Azimuth stacks with an orientation parallel to the fractures tend not to show these spectral notches – allowing for another way to detect the fracture orientation.

In the second method we analyze the seismic data in the frequency-wavenumber (FK) domain. In our studies on the scattering effects of discrete fractures on synthetic seismic data we have observed the presence of both forward and backscattered signals. In particular, the backscattered signals are at a maximum when the acquisition direction is normal to the fractures and a minimum when the direction is parallel to the fractures. In the FK domain we can separate the backscattered energy and determine the fracture spacing from its dominant wavenumber. FK analysis for fracture spacing estimation was successfully applied to numerical model results for both PP and PS converted waves. Because S wave arrivals have shorter wavelengths than P waves, PS arrivals have higher resolution and therefore can provide estimates of finer scale fracture spacing (Zhang et al., 2006).

Field Example

The Emilio Field is a fractured carbonate reservoir located in the Adriatic Sea in about 80m of water. The field is an area of complex folding and faulting at a depth of approximately 2800m, and a high quality 3D/4C seismic survey was acquired using ocean bottom cables (OBC) (Vetri et al., 2003; Gaiser et al., 2002). Scattered wave analyses of these data have been presented in previous papers (e.g., Willis et al., 2004, 2005, 2006; Zhang et al., 2006), while other analyses have been reported elsewhere in the literature (e.g., Vetri et al., 2003; Gaiser et al., 2002).

Scattering analysis for fracture orientation estimation was applied to the Emilio data using stacks of the near to mid range (< 3500 m) offsets of the preprocessed PP data (Vetri et al, 2003) in eighteen different azimuth orientations from East to West. A 20-degree wide set of overlapping windows was used with a 10 degree step size (note that these angle ranges include the corresponding ranges 180 degrees away). This process created eighteen 3D stacked volumes. Figure 10 shows two common shot gathers from the data, one oriented normal and the other parallel to the maximum horizontal stress direction as determined from borehole breakouts and FMI logs (Vetri et al., 2003). These gathers are compared to gathers with the same orientations from the numerical modeling results. The field data oriented normal to the expected fracture strike shows more backscattered energy. This consistency between numerical model, laboratory physical modeling (Figure 3), and field data is quite striking and gives us confidence in applying the Scattering Index method to these data.
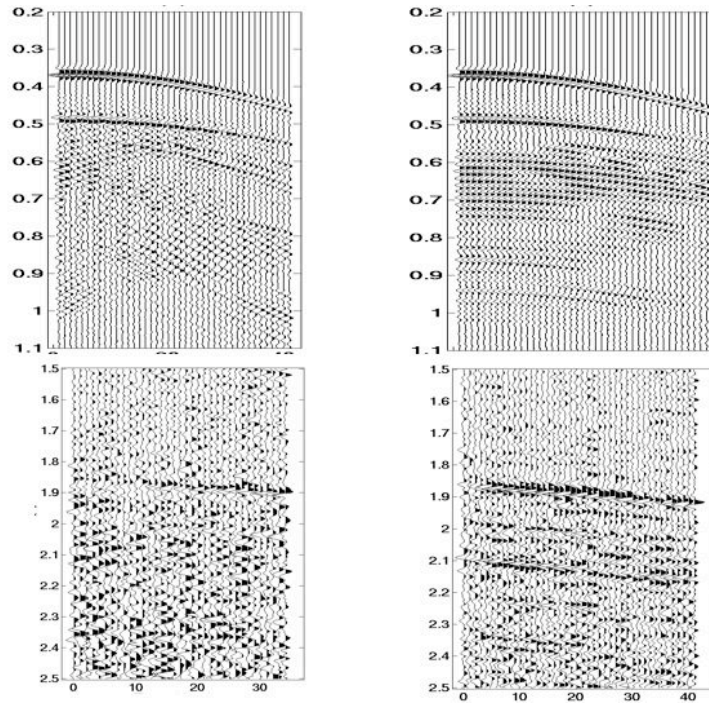
Figure 10 Top panels show the numerical modeling common source gathers for a set of parallel fractures with 50m spacing (normal to fractures on the left, parallel to fractures on the right). Bottom panels show two azimuthal source gathers from the Emilio field data, with the left panel being oriented normal to the expected fracture direction and the right panel being oriented parallel to the fracture direction.

The transfer functions and scattering indices for the formation zone were computed for each of these azimuthal stacked volumes (e.g., Willis et al., 2006). The scattering indices were sorted and directions for those with the highest angular contrast in scattering index values were plotted as 'quivers' (i.e., short line segments) giving a map view of the location and direction of possible fracture zones. We then performed a map migration of all the scattering indices to correctly position them in space. The results show a very strong correlation between the spatial distribution and orientation of our fracture results and the fault system in the field (Figure 11). We observe that the zones of high fracture density tend to congregate around the fault zones, particularly near multiple faults and at fault tips. In addition, we see that the quivers tend to align either parallel or perpendicular to the faulting. The FK and spectral notch methods were also applied to the Emilio data to estimate fracture spacing. Both methods resulted in fracture spacing estimates of 25-40m. Validation of these values is difficult since there is no ground truth information for comparison, however the consistency of the estimates from the different methods provides some confidence. The spacing estimates are plotted in the center panel of Figure 11.
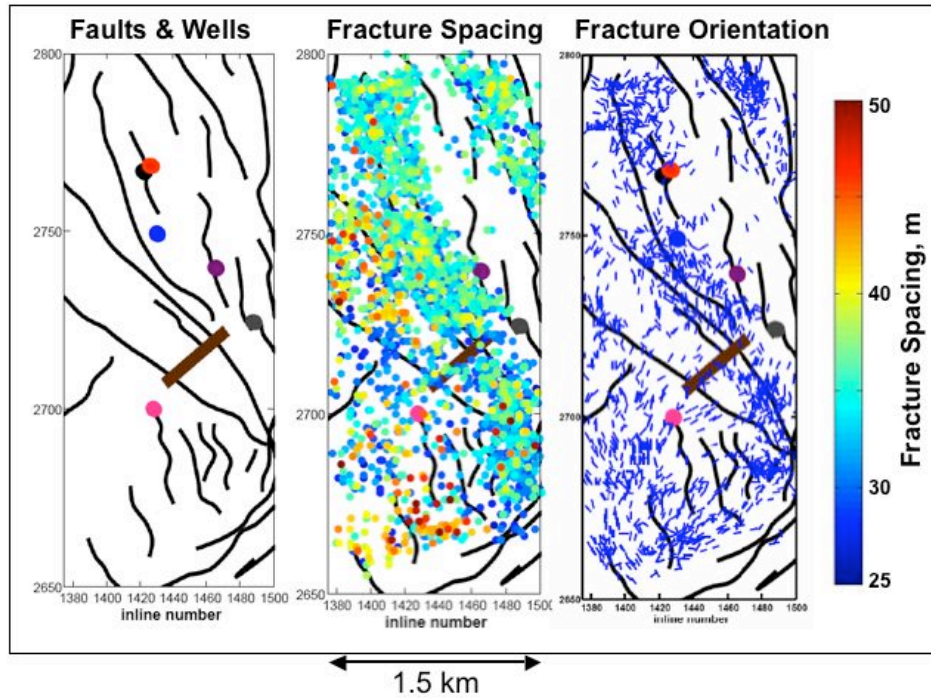
Figure 11 Scattering analysis results for the Emilio field. The left panel shows the interpreted fault locations (black lines) and the well positions (colored circles). The right panel shows the map migrated scattering index quivers. The distribution of the quivers is an estimate of the fracture density in the field, while the orientation of the quivers gives an estimate of fracture orientation. The center panel shows the fracture spacing estimates obtained from spectral analysis of the scattered wave energy.

These fracture directions are comparable to those derived by shear wave anisotropy (Vetri et al, 2003) and with available well information (Willis et al., 2006). Figure 12 compares well-derived fracture orientations with those derived by the scattering index analysis. The top row shows the well information (from Vetri et al., 2003) indicating the direction of the maximum horizontal stress (SHmax). In general, fractures align subparallel to the SHmax direction. We added a red arrow to the Well 4 results to emphasize the SHmax direction, since break out directions tend to align in the SHmin direction. The middle row shows close-ups from Figure 11 around these three wells. To further clarify the fracture trends, we histogrammed the map migrated scattering directions around each well and plotted them in rose diagram format in the bottom row of Figure 12. There is very good agreement between the scattering index orientations and the well-derived fracture orientations at these three wells. Willis et al. (2006) provides a more complete review of the method and results.
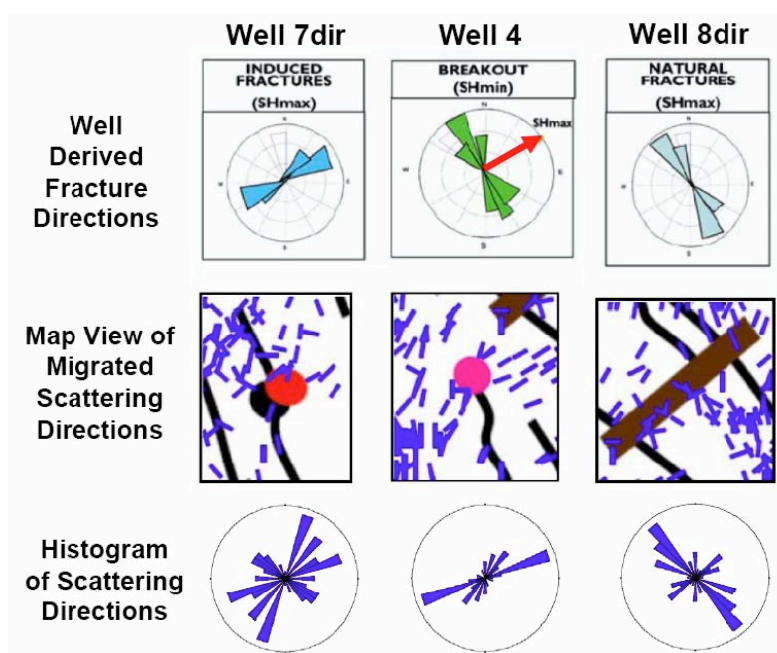
Figure 12. The top set of diagrams show the well derived fracture information (from Vetri et al., 2003) – SHmax is generally the direction of fracture strike. The red arrow indicates the direction of SHmax for well 4. The middle three diagrams are close-ups of Figure 23 around the corresponding well locations showing the agreement of the map migrated scattering directions with the well fracture directions. The bottom three diagrams show the histograms, in rose diagram format, of the map migrated scattering index directions around each of the wells (from Willis et al., 2006).

Conclusions

Major fracture corridors in the subsurface will scatter seismic energy, and by analyzing these scattered wave signals (which are often treated as noise and discarded or removed in most processing approaches) the orientation of the fracture corridors can be estimated. Spectral analysis of these signals can also provide information on the fracture spacing or density. Numerical modeling, laboratory physical modeling, and field data analysis indicate that backscattered energy is maximized when the acquisition direction is normal to the fracture strike direction. When the acquisition direction is parallel to the fracture strike direction, only forward scattered energy is generated. As a result, scattered wave energy is preferentially enhanced when stacking data acquired parallel to fractures. The Scattering Index method (Willis et al., 2006) is one approach to extracting fracture orientation information from these scattered signals. Because this is a differential method that compares the seismic wavelet above and below some interval of interest, any overburden complications or acquisition footprint will be minimized. The method can also fit quite easily into normal processing flows since it is based on standard deconvolutional methods. Although we've described the method in terms of the analysis around a 'zone of interest' in the subsurface, the method could also be used in a more generic exploration mode where a moving set of windows separated by some number of time samples could be applied to the full trace within azimuthal gathers to generate

Scattering Index values as a function of depth (travel time) with the subsurface as well as spatially as we showed in this paper.

Our methods for estimating fracture orientation and fracture spacing from the seismic scattering signals have been tested with numerical modeling data and field data from several different fields, both onshore and offshore. The fracture orientation results have been validated against available well log measurements (FMI logs), other seismic analysis methods, and existing geologic models of the fields and are quite promising.

Acknowledgements

References

Aki, K., and B. Chouet, 1975, Origin of coda waves: source, attenuation, and scattering effects, J. Geophys. Res., 80, 3322-3342, 1975

Coates R.T. and Schoenberg, M., 1995, Finite difference modeling of faults and fractures, *Geophysics*, 60, 1514-1526.

Frankel, A. and Clayton, R.W., 1986, Finite difference simulations of seismic scattering: implications for the propagation of short-period seismic waves in the crust and models of crustal heterogeneity, J. Geophys. Res., 91, 6465-6489.

Gaiser, J., Loinger, E., Lynn, H, and Vetri, L, 2002, Birefringence analysis at the Emilio field for fracture characterization, *First Break* v 20, 505-514.

Groenenboom, J., and J. Falk, 2000, Scattering by hydraulic fractures: Finite-difference modeling and laboratory data: Geophysics, **65**, no.2, 612-622.

Jannaud, L.R., Adler, P.M., and Jacquin, C.G., 1993, Spectral analysis and inversion of experimental codas, *Geophysics*, 58 (3), 408-418.

Luo, M., and B.J. Evans, 2004, An amplitude-based multiazimuth approach to mapping fractures using P-wave 3D seismic data: Geophysics, **69**, no.3, 690-698.

Lynn, H., Simon, K. M., and Bates, C. R., 1996, Correlation between P-wave AVOA and S-wave traveltime anisotropy in a naturally fractured gas reservoir, *The Leading Edge, 15,* 931-935.

Mallick, S., Craft, K.L., Meister, L.J., and Chambers, R.E., 1998, Determination of the principal directions of azimuthal anisotropy from p-wave seismic data. *Geophysics*, v. 63, 692-706.

Nakagawa, S., Nihei, K., and Myer, L., 2002, Numerical simulation of 3D elastic wave scattering off a layer containing parallel periodic fractures: 72nd Annual International Meeting. SEG, Expanded Abstracts.

Nakagawa, S., Nihei, K., and Myer, L., 2003, Three-dimensional elastic wave scattering by a layer containing vertical periodic fractures: J. Acoust. Soc. Am, **13**.

Nihei, K., Nakagawa, S., Myer, L. and Majer, E., 2002, Finite difference modeling of seismic wave interactions with discrete, finite length fractures: 72nd Annual International Meeting. SEG, Expanded Abstracts.

Pyrak-Nolte, L., 1996, The seismic response of fractures and the interrelations among fracture properties, Intl. J. Rock Mech. And Min. Sci. and Geomech. Abs., v.33, no.8, p. 785-802.

Rüger, A., 1998, Variation of P-wave reflectivity with offset and azimuth in anisotropic media: *Geophysics*, 54, 680-688.

Saenger, E. H., Gold, N. and Shapiro, S. A., 2000, Modeling the propagation of elastic waves using a modified finite-difference grid, *Wave Motion*, 31, 77-92

Sato, H., and M. Fehler, 1998, Seismic wave propagation and scattering in the heterogeneous Earth, American Institute of Physics Press.

Schultz, C. and M.N. Toksöz, Reflections from a randomly grooved interface: ultrasonic modelling and finite difference calculation, Geophys. Prospecting, 43, 581-594, 1995.

Vetri, L., Loinger, E. Gaiser, J. Grandi, A., Lynn, H, 2003, 3D/4C Emilio: Azimuth processing and anisotropy analysis in a fractured carbonate reservoir, *The Leading Edge*, 675-679.

Vlastos, S., Liu, E., Main, I. G. and Li, X.Y., 2003, Numerical simulation of wave propagation in media with discrete distributions of fractures: effects of fracture sizes and spatial distributions: Geophys. J. Int., **152**, 649-668.

Willis, M., Rao, R., Burns, D., Byun, J., Vetri, L., 2004, Spatial orientation and distribution of reservoir fractures from scattered seismic energy, *74th Annual SEG Meeting, Expanded Abstracts*.

Willis, M., Rao, R., Burns, D., and Toksoz, M. N., 2005, Fracture spacing and orientation estimation from spectral analyses of azimuth stacks, Expanded abstract, EAGE meeting, Madrid.

Willis, M., Burns, D. R., Rao, R., Minsley, B., Toksoz, M. N., Vetri, L., 2006, Spatial orientation and distribution of reservoir fractures from scattered seismic energy, *Geophysics, v.71, 5, p 043-051*.

Zhang, Y., Campman, X., Grandi, S., Chi, S., Willis, M. E., Toksoz, M. N, Burns, D. R., F-K domain characteristics of the seismic response of a set of parallel discrete fractures, expanded abstract, 76th SEG Annual Meeting, 2006